European Review for Medical and Pharmacological Sciences 2022; 26: 7580-7593

An *in silico* analysis of the impact *of POLE* mutations on cladribine docking

L. LOGANATHAN[1], A. AL-HAIDOSE[2], A. GANESH KUMAR[3], L.B. SUJATHA[4], F.H. CARLUS[4], A. ALHARBI[5], S. ALHYASSAT[6], K. MUTHUSAMY[1], S.J. CARLUS[7], A.M. ABDALLAH[2]

[1]Department of Bioinformatics, Alagappa University, Karaikudi, Tamil Nadu, India
[2]Department of Biomedical Sciences, College of Health Sciences, QU Health, Qatar University, Doha, Qatar
[3]Department of Microbiology, Center for Research and Development, Hindustan College of Arts and Science, Padur, OMR, Chennai, India
[4]Department of Zoology, Pachaiyappa's College, E.V.R. Periyar Road, Shenoy Nagar, Chennai, India
[5]Cardiogenetics Unit, Pediatrics Department, College of Medicine, Taibah University, Al-Madinah, Saudi Arabia
[6]Department of Laboratory Medicine and Pathology, Hamad Medical Corporation, Qatar
[7]Genetics and Genomics Laboratory, Micro Health Laboratories, Doha, Qatar

Abstract. – OBJECTIVE: Polymerase ε exonuclease (POLE) is an enzyme involved in DNA replication and may be an attractive therapeutic target in various cancers. Here we sought to model the impact of specific *POLE* mutations on protein function. Due to the lack of a crystal structure, the tertiary structures of the wild type and four common mutants were modeled using I-Tasser server.

MATERIALS AND METHODS: Molecular docking and dynamic simulation studies were performed, and the structure and function of the mutants analyzed through residue conservation analysis and protein folding energy changes.

RESULTS: All mutants of *POLE* gene had favorable binding affinities compared with their wild type of counterpart. The P286R variant, but not the other variants, disrupted cladribine binding to the protein. Similarly, dynamics studies revealed instability of the P286R mutant, while V411L, L424V, and L424F appeared to favor cladribine binding.

CONCLUSIONS: Since P286R is a hotspot mutation in endometrioid carcinomas, patients with this variant may not respond to cladribine. Population-based pharmacogenomics studies will be required to validate our results.

Key Words:
Molecular docking, Molecular dynamics, Residue conservation, Mutation, POLE, SNP, Gynecology cancer.

Introduction

DNA polymerase epsilon (POLE) is a B-family DNA polymerase that plays an important role in leading strand synthesis in nuclear DNA replication[1]. The enzyme has four subunits: p261 (POLE), p59 (POLE2), p17 (POLE3), and p12 (POLE4). p261, encoded by the polymerase ε exonuclease (*POLE*) gene, has a conserved polymerase exonuclease domain (ED), a proofreading domain responsible for detecting and removing mis-incorporated nucleotides[2]. Defects in the proofreading function of the POLE enzyme contribute to genomic instability in different cancers[3]. All reported somatic and germline *POLE* mutations are heterozygous and no loss of heterozygosity has been reported[3]. Although they exist in heterozygous form, the pathogenicity of these mutations remains unclear and the role of these mutations on tumor development is not explained[4]. It has been recently shown[5] that different *POLE* mutant alleles differentially influence and drive tumor mutation burden, thereby dividing patients into distinct subgroups. Interestingly, all *POLE* mutations reported in patients with ultra-mutated tumors are located in the proofreading ED. *POLE* is frequently mutated in different solid cancers and leukemias[6], with 92 *POLE* ED mutations reported in different cancers according to the cBioPortal database (available at: https://www.cbioportal.org/, accessed in November, 2021)[7,8].

Cladribine (2-chlorodeoxyadenosine; 2-CdA) is a nucleoside analogue developed nearly 50 years ago and is now commonly used to treat variety of tumors[9] and individuals with multiple sclerosis due to its immunosuppressive activity[10].

Corresponding Author: A.M. Abdallah, MD; e-mail: aabdallah@qu.edu.qa

Cladribine is activated after undergoing sequential intracellular phosphorylation, which leads to the accumulation of its active form 2-Cd-ATP[9]. 2-Cd-ATP incorporates in DNA strands, thereby inhibiting enzymes involved in DNA synthesis, including POLE[11,12]. Interestingly, *in vivo*, cancers with *POLE* mutations show hypersensitivity to nucleoside analogues compared with *POLE* wild type tumors, suggesting that nucleoside analogues may be an effective therapeutic strategy in patients with advanced-stage *POLE*-mutant cancers[13].

Here we focused on common mutations reported in *POLE* gene including *P286R*, *V411L*, *L424V*, and *L424F* of *POLE* gene. These somatic mutations cluster in the exonuclease proofreading domain of *POLE* gene and are found in tumor tissue from different cancers, such as endometrial (around 8% of patients) and colorectal (around 3% of patients)[5,14]. Patients with *P286A* and *L411V* are associated with high tumor mutational burdens (≥100 mutations per megabase), and while tumors harboring *L424F* mutations are also associated with high tumor mutational burdens, *L424V*-mutant tumors have lower mutational burdens (5-10 mutations per megabase)[4]. The crystal structures of target proteins are crucial for the theoretical analysis of protein structure and function but, when the structure in unavailable, the tertiary structure must be predicted through homology modeling or *ab initio* modeling based on available template structure data. To predict the deleterious effects of these four recently reported mutations[15], protein tertiary structures were modeled through *ab initio* protein modeling, and the predicted structure was mutated manually to obtain individual structures for further processing. Several computational analyses and validations were performed to understand the impact of structural changes on protein function and drug binding. We selected cladribine as a reference drug molecule for docking studies[9,16]. In addition, amino acid conservation and impact of the variants on protein folding were analyzed.

Materials and Methods

Selection of SNPs

POLE encodes the catalytic subunit of DNA polymerase ε and is involved in nuclear DNA repair and replication[17]. The most common *POLE* mutations are found within the ED (exons 9-14), important for proofreading during DNA replication. These mutations result in an extremely high mutational load and the hypermutated phenotype in colorectal and endometrial carcinomas[18]. The most prevalent *POLE* mutations reported in endometrial carcinoma patients are P286R, V411L, L424V, and L424F, with two variants (P286R and V411L) accounting for 63-76% of all *POLE* point mutations. *POLE* mutations have long been known to be associated with improved long-term progression-free survival[19].

In Silico Protein Structure Modeling of Non-Synonymous (Ns)Snps

The protein structures of wildtype and mutant *POLE* were modeled using Maestro (Schrödinger, New York, NY). Before mutating the protein, we confirmed the mutation position and mutated residues in Uniprot (KB_Q07864). After introducing the mutations, the models were optimized, and the energy reduced using the OPLS3 forcefield in Maestro. The root mean square deviation (RMSD) for each energy-minimized mutant protein was computed in relation to the wild-type protein structure[20]. The optimized structure was used in further docking studies after minimization (Figure 1).

Meta-Study of Target Snps

A meta-study gathers previously reported information about selected variants and their specific deleterious effects in genetic disorders as determined by case-control studies conducted in a different ethnic populations[21]. Table I details the *POLE* variants previously reported to be deleterious.

Active Site Prediction

The SiteMap module in Schrödinger was used to identify the most favorable binding regions in the protein's active site[22] on the basis of hydrophobic, hydrophilic, and charged amino acids in the tertiary protein structure (Figure 2). A customized grid was generated with co-ordinates in three axes, and the ligand-receptor interaction distance was fixed at ≤ 20 Å. Receptor grid generation was implemented to create a fine grid covering the active site. Cladribine was docked with the four variant models and one wildtype protein in extra precision mode (XP).

Protein-Ligand Docking

The selected drug cladribine was obtained from the PubChem database as a ligand for docking experiments, with which we generated conformers using Ligprep in Maestro utilizing the

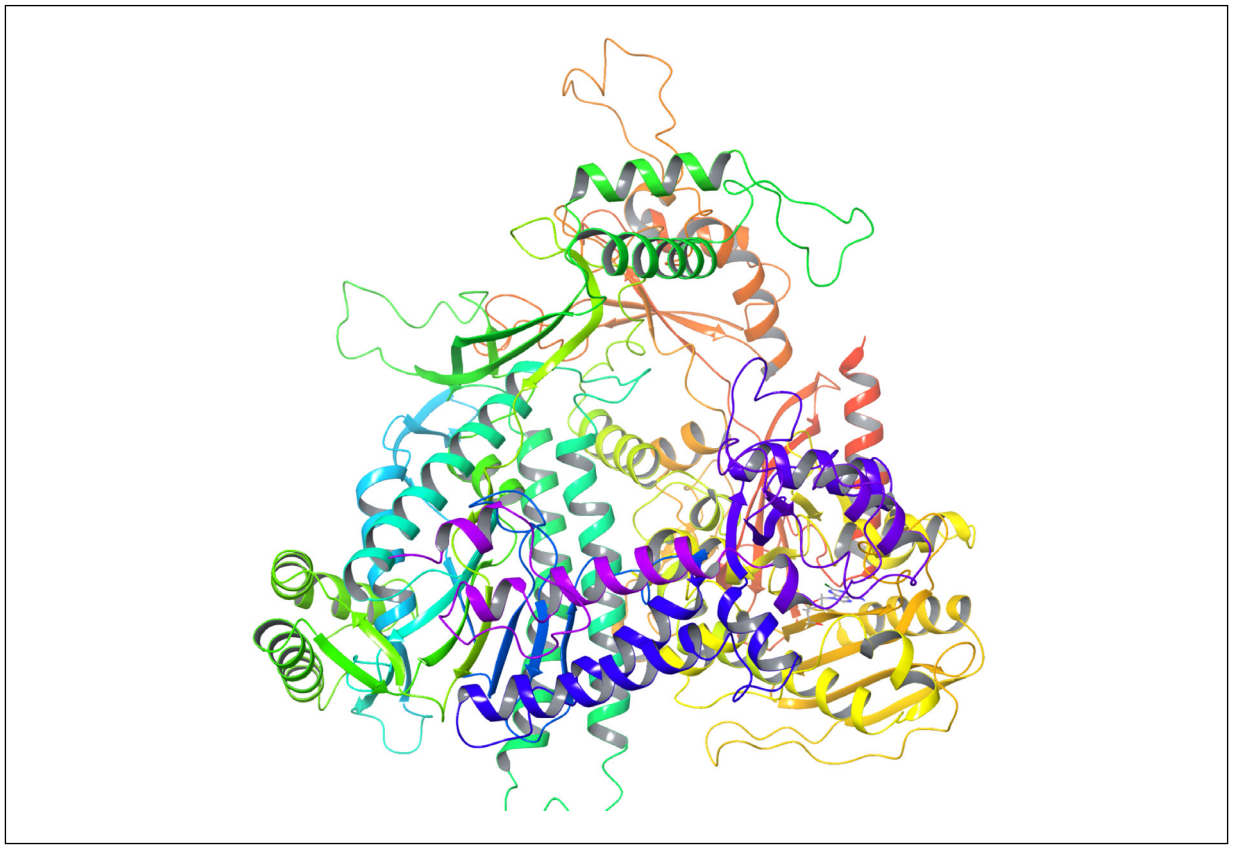

Figure 1. Energy-minimized tertiary structure of POLE protein.

OPLS3 forcefield. Among the different conformers of cladribine, a molecule with high binding affinity was determined *via* molecular docking using Glide in Maestro[23,24]. The active site was defined based on the best active site predicted by SiteMap in the protein structure. After completing the docking protocol, the docked ligands were carefully studied for binding pose selection.

Secondary Structure Prediction

To identify structural alterations induced in the target protein by the missense mutations[25] and, as

Table I. Detailed information about the POLE variants studied.

Variants/SNP	Alleles	Clinical significance	Transcript ID	Pathogenicity Prediction	Evidence
rs1057519945 V411L	C/A/T	Likely pathogenic	ENST00000320574.10	Polyphen – Probably Damaging SIFT – Deleterious	Phenotype evidence available, Cited
rs1057519943 P286R	G/C/T	Likely pathogenic	ENST00000320574.10	Polyphen – Probably Damaging SIFT – Deleterious REVEL – Pathogenic	Phenotype evidence available, Cited
rs483352909 L424F	G/A/C	Pathogenic	ENST00000320574.10	Polyphen – Probably Damaging SIFT – Deleterious REVEL – Pathogenic	Frequency, identified in ExAC, gnomAD consortium, phenotype evidence available, Cited
rs483352909 L424V	G/A/C	Pathogenic	ENST00000320574.10	Polyphen – Probably Damaging SIFT – Deleterious REVEL – Pathogenic	Frequency, Identified in ExAC, gnomAD consortium, phenotype evidence available, Cited

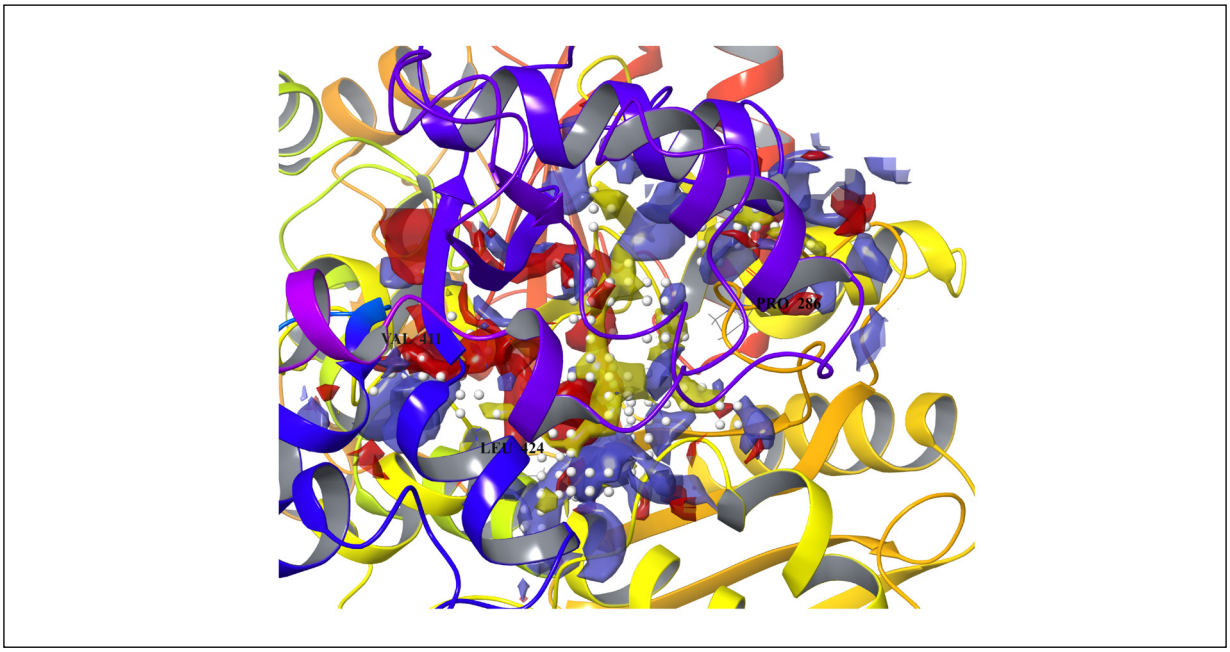

Figure 2. Protein tertiary structure focusing on the active site of the target molecule. Yellow regions are hydrophobic, red regions are hydrophilic and charged.

a consequence, any functional change, the protein sequence encoded by *POLE* was retrieved from UniProtKB and individual sequence files with variant modifications prepared for comparison of protein secondary structure. MAFFT alignment v. 7.0 was used to align the modified sequences[26] using the BLOSUM 62 scoring matrix as a scoring function. The secondary structure of the aligned sequences was generated using Geneious R 6.1.2 (Biomatters, Auckland, New Zealand)[27].

Binding Energy Calculations

In addition to Glide energy, the binding energy of the docked complex was calculated using Prime MM-GBSA in Schrödinger since these results are important in the design of new drug molecules specific to the target protein molecule. Prime MM-GBSA was used to calculate the binding free energy of the studied molecules, the molecule's strain energies, and the binding energies of the ligand and receptor.

Molecular Dynamic Simulation (MDS)

Desmond in Maestro was used for MDS using the OPLS 3 forcefield. All essential steps were carried out as previously[28,29]. The box dimension ensured that the protein's atoms would be in a suitable area distant from the box's wall with periodic boundary conditions. The system was solvated using the SPC water model and initially equilibrated with NVT, NPT followed by a 100 ns final molecular dynamics equilibration simulation. All trajectories were saved at every 2 ps for further analysis.

Residue Conservation Analysis

The amino acid sequence of *POLE* was retrieved from UniProtKB and used as the source file for conservation analysis. The conservation score of each amino acid was predicted through multiple sequence analyses using Consurf Server (available at: https://consurf.tau.ac.il/consurf_index.php) using the default settings, Bayesian cal-

Table II. Information about the POLE protein and candidate drug, cladribine.

Protein name	Gene name	Amino acid length	Template structural information	Variants identified as disease-causing	Available drug information
DNA polymerase epsilon catalytic subunit A	POLE	2286 aa target area (250 to 450)	X-ray crystal structure (5VBN) sequence coverage - 2,142 to 2,286 [31]	V411L P286R L424V/F	Cladribine [14]

culation, and the HMMER homology search algorithm. Conserved amino acids were identified after scoring from 1 to 9, with a higher score denoting higher conservation[30]. Furthermore, amino acid function was predicted based on position in the protein, i.e., buried or exposed.

STRUM Prediction

The STRUM server[31] was chosen to identify structure-dependent changes in protein stability based on the point mutations. Scores below zero indicated protein destabilization, while those above zero indicated that the mutation stabilized the protein structure. In this way, changes to the active site that might alter drug binding affinity were identified.

Results

The studied *POLE* mutations were predicted to be deleterious *in silico* and have been shown to be disease-causing experimentally[14] (Table II). The POLE protein studied here is described in Table II. Since the crystal structure of the POLE protein was not publicly available, a significant template structure of 5VBN was identified through homolog screening using the BLAST tool from the NCBI.

Amino Acid Conservation Analysis

The predicted energy changes in protein folding on introduction of the mutations were between 3.56 and -2.81 (Table III). The ConSurf server also helps to predict amino acid nature and conservation through sequence alignment and analysis (Figure 3). Table IV shows the conservation score of each mutation and its predicted function. All the mutated amino acids were highly conserved, with *P286R* buried and categorized as a functional residue and the other mutants exposed and categorized as structural. Among the four variants, *P286R* had a STRUM score of -2.81, suggesting that this variant might influence the protein structure.

Secondary Structure Analysis

We next examined secondary structural changes caused by the four SNP sequence variants. The addition and loss of secondary structural elements were observed near the mutated regions (Figure 4). *V411L* induced turn loss and helix gain around the mutation; *L424V* showed no change in turns near the mutated site; *L424F* showed secondary structure displacement through a specific turn replaced with a small helix at the mutated site, while P286R produced several secondary structural changes at the mutant site such as loss of the turn and loop region and formation of a helix. Therefore, all four variants resulted in structural changes in the protein secondary structure.

Table III. STRUM server predictions for the identified variants.

Variant	Score ΔΔG (ddG)	Remarks
V411L	2.36	Stabilized
P286R	-2.81	Destabilized
L424F	3.34	Stabilized
L424V	3.56	Stabilized

Molecular Docking Analysis

All mutant and wildtype protein structures underwent energy optimization during pre-docking experiments. Cladribine was docked in the active sites of the five proteins in parallel and binding affinities and conformational changes compared to understand the impact of the drug in the presence of specific mutations (Table V). The wildtype protein had a glide score of -7.13 kcal/mol in the presence of cladribine. The *L424V/F* and *V411L* mutants had higher glide scores of -8.08 and -8.04 kcal/mol, respectively, while P286R had a lower score of -5.89 kcal/mol, indicating reduced binding affinity. The glide scores are a direct measure of binding affinity of molecules in protein active sites. The binding energy ranged from -51.94 to -36.24 kcal/mol, and Asp462, Thr278, Gln277, Arg1077, and Ser1075 were interacting residues. Of these, Thr278 and Gln277 were hotspot residues favoring binding between the molecules (Figure 5).

Molecular Dynamic Simulations

All the docked protein-ligand complexes were used to prepare topology and coordinate files for MD simulations in Desmond. In the biological setting, the predicted tertiary protein structure is extremely dynamic and structural stability is highly important for predicting the target protein function. For the modeled or mutated protein, the RMSD is an important parameter when determining protein stability. We therefore performed molecular simulation of the docked complex molecule for 100 ns to determine and differentiate native and mutant structures.

Root Mean Square Deviation

Structural changes in the studied complexes were measured from 0 ns to 100 ns. RMSD plots

Figure 3. Color-coded sequence alignment indicates sequence conservation at the sites of the studied mutations.

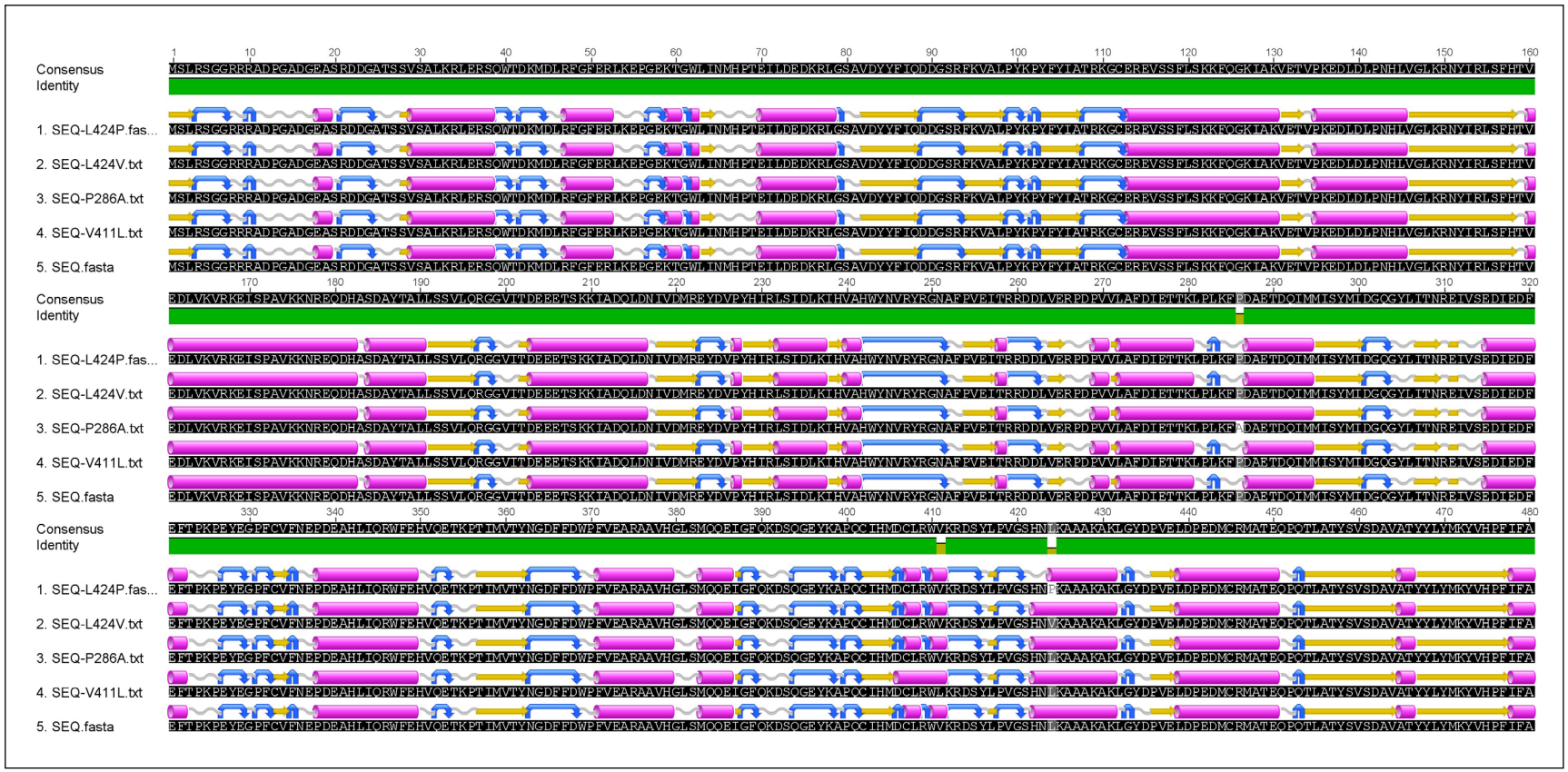

Figure 4. Secondary structure prediction of the POLE wild and mutant sequences.

Table IV. Residue conservation analysis and function prediction by ConSurf analysis.

Variants	Color scale, score	Buried/exposed	Function
V411L	Highly conserved, 9	Buried	Structural
P286R	Highly conserved, 9	Exposed	Functional
L424F	Highly conserved, 9	Buried	Structural
L424V	Highly conserved, 9	Buried	Structural

show the deviation of the backbone atoms of the protein residues observed throughout the simulation (Figure 6). The wildtype protein RMSD was stable at 0.31 nm (3.1 Å), while the mutants were stable at 0.22 to 0.39 nm (2.2 to 3.9 Å), indicating that the mutations in structural residues significantly altered system stability with respect to RMSD values represented in the RMSD plots (Figure 6). The RMSD changes indicated that the protein structures or their conformational patterns were unstable.

Protein Residue Fluctuation

Protein function can be altered by docking chemicals or drug molecules to hotspot sites in the protein molecule. The *P286R* SNP was very unstable and reduced drug binding affinity. In molecular dynamics simulations, this mutant decreased the RMSF stability by 0.38 nm (3.8 Å) and interactions with cladribine were lost (Figure 7). Important and strong non-covalent interactions between the amino acid residues and atoms of the drug molecule will improve stability and affinity, and indeed the other mutants retained interactions and stability in simulations. Residue fluctuation near the loop regions is expected and influences the structural conformation.

H-Bond Analysis

Hydrogen bond analysis showed a loss and gain of hydrogen bonds in each trajectory throughout the simulations. Important and strong non-covalent interactions between the amino acid residues and atoms of the drug molecule improve stability and affinity, and indeed the other mutants retained interactions and stability in simulations. There were very few hydrogens bond networks in the *P286R* variant model, while the other models showed considerable interactions maintaining complex stability. To simplify the data, we present wild and mutant *L424F* in Figure 8, which shows that the *L424F* model has the most H-bond interactions, while the wildtype protein and other mutants had fewer H-bonds throughout the simulation. The wildtype model showed stable interactions including H-bonds, hydrophobic interactions, and salt bridges, while *L424F* had more important residue interactions such as with Thr278, Tyr362, His422, and Arg976 *via* all the major possible contacts.

Discussion

The computational studies on *POLE* gene mutation brings out the significant outcomes based on the several *in silico* analysis on specific SNPs on the protein structure. The amino acid conservation analysis differentiates the studied SNPs based on their residue conservation score obtained from sequence alignment (Figure 3). Furthermore, the conserved residues were categorized as structural and functional with respect to their position in the protein structure. Associate results were observed in secondary structure analysis. All the studied mutations have substantial secondary structure changes near the mutated regions (Figure 4). All the studied variants impact protein structure and

Table V. Molecular docking results of cladribine in the wild and mutated structures.

Molecule	Glide XP score (kcal/mol)	Binding energy (kcal/mol)	Interacting residues (H-bonds)
Protein_Wild	-7.139	-41.567	Asp462, Thr278
Protein_V411L	-8.044	-49.590	Gln277, Thr278
Protein_P286R	-5.894	-36.241	Arg1077, Ser1075
Protein_L424V	-8.080	-51.623	Gln277, Thr278
Protein_L424F	-8.080	-51.947	Gln277, Thr278

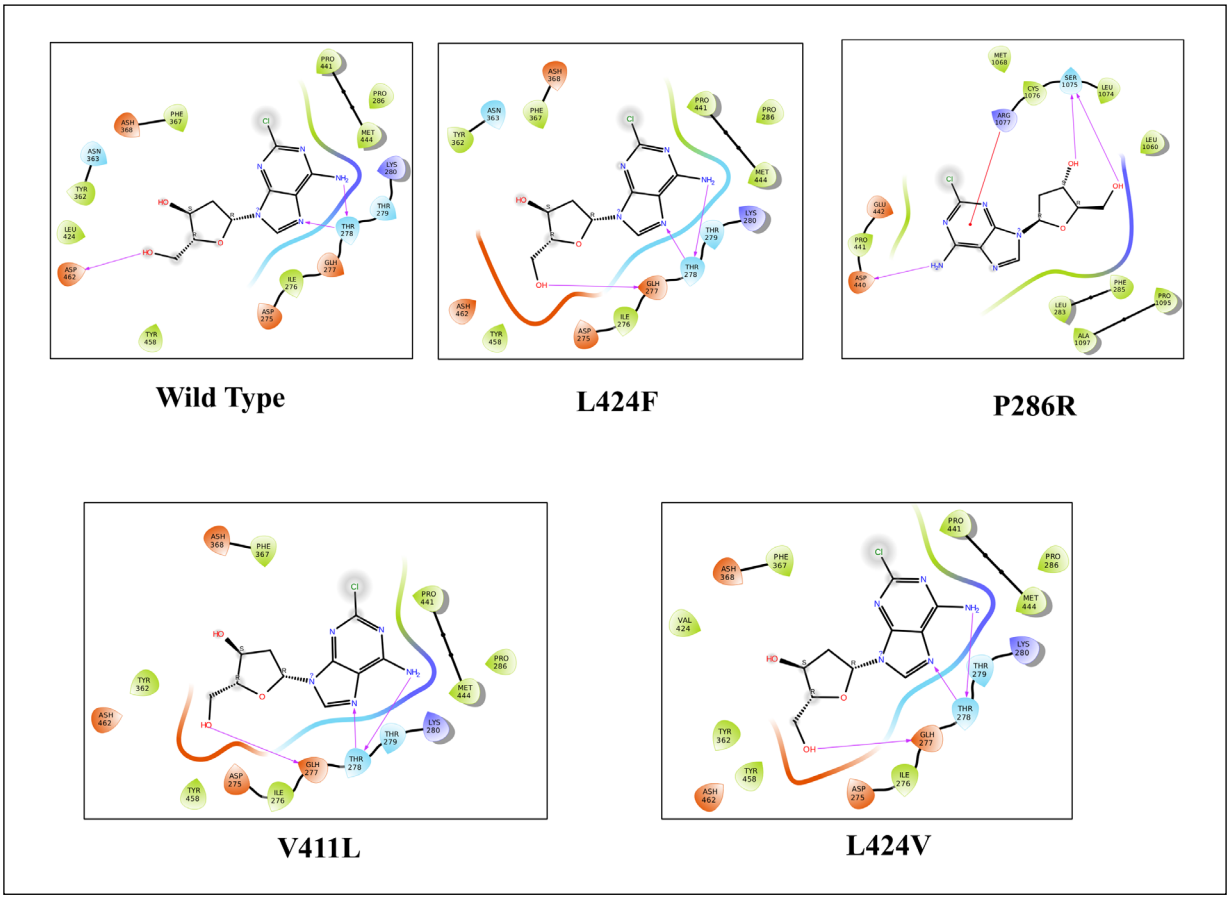

Figure 5. Molecular docking studies revealed 2-dimensional interactions of the drug molecule in the protein active site.

may, therefore, alter protein function. The superimposition of wild and mutant structures revealed significant differences in structure between mutants and wildtype, especially for the *P286R* mutant. These observations confirm the negative impact of the variants on protein stability and conformation. The mutated structures induced significant differences in structural alignment and conformational state of the functional protein in three-dimensional views.

The molecular docking analysis reveals that the Cladribine drug molecule's binding nature to the active POLE protein is altered. The protein structure with specific mutation differentiates the drug binding affinity and binding energy. Among them, P286R has a significant reduction in binding score compared to wild type. It indicates that the P286R mutation disrupts the binding cavity and leads to an unfavorable binding compatibility with the drug molecule. Furthermore, RMSD, RMSF, and hydrogen bond analysis from molecular dynamic simulation studies reveal several supporting data. The mutants have an important role in the structural stability, as well as in functional and conformational variation of the protein. The P286R has an unstable structure and very few hydrogen bonds are observed throughout the 100 ns simulation time. Overall, it is clearly assumed that the studied mutants have a crucial role in modulating the function of the *POLE* gene.

Conclusions

Here we performed *in silico* analyses to explore the impact of common *POLE* variants on protein structure, function, and drug binding. Docking studies showed that all mutations altered interactions with cladribine, which may alter drug efficacy depending on the mutation and its position. Structural stability and hydrogen bond interactions demonstrated that the mutations significantly contributed to changes in drug affinity. Of the studied variants, *P286R* had the greatest impact and resulted in structural instability and reduced binding affinity. The theoretical prediction of differential binding between cladribine and dif-

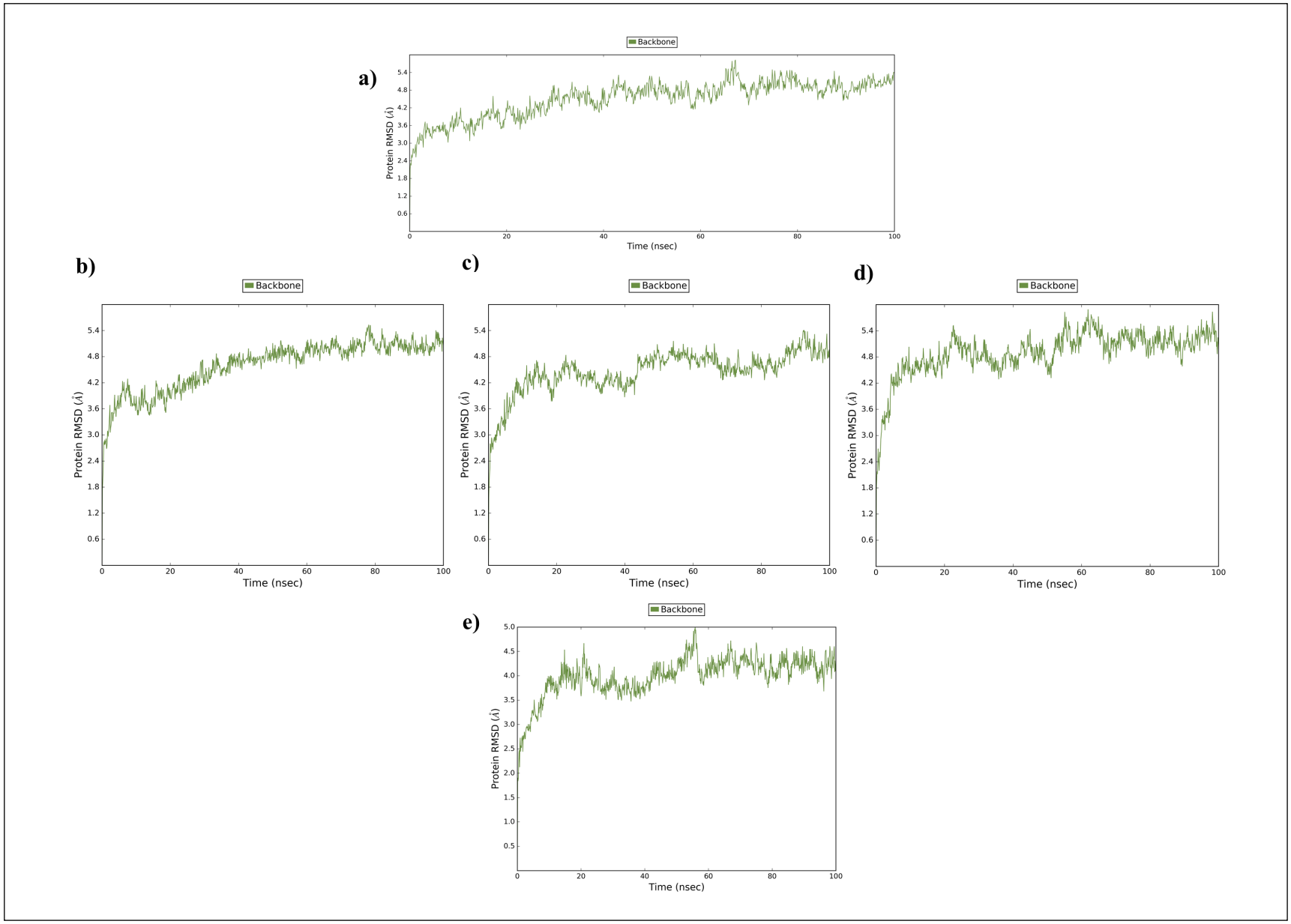

Figure 6. Molecular dynamics simulations and RMSD values indicate structural stability: **a**, wildtype; **b**, L424F; **c**, P286R; **d**, V411L; **e**, L424V.

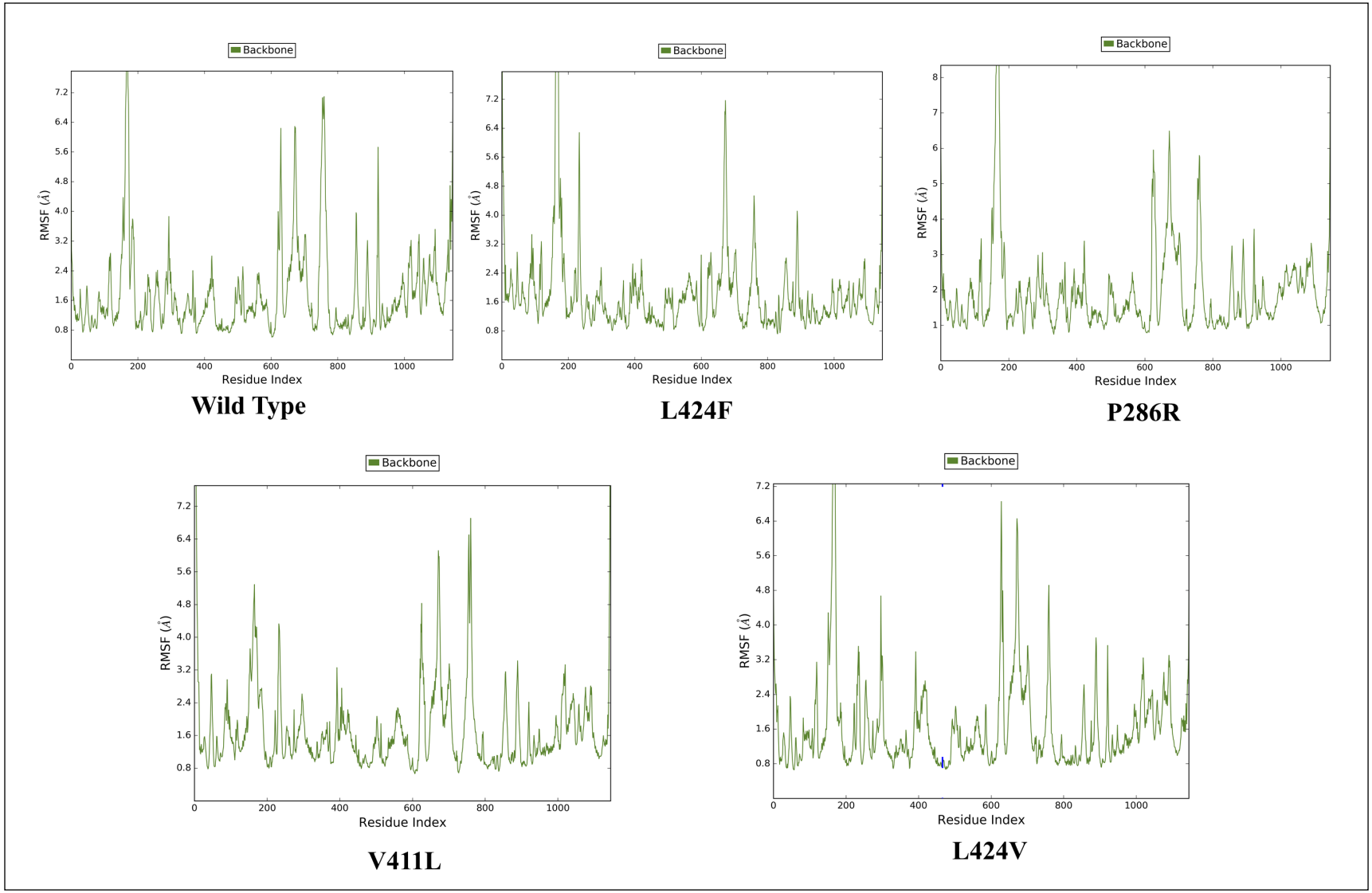

Figure 7. RMSF plots showing the residue fluctuation in wildtype and mutant protein structures.

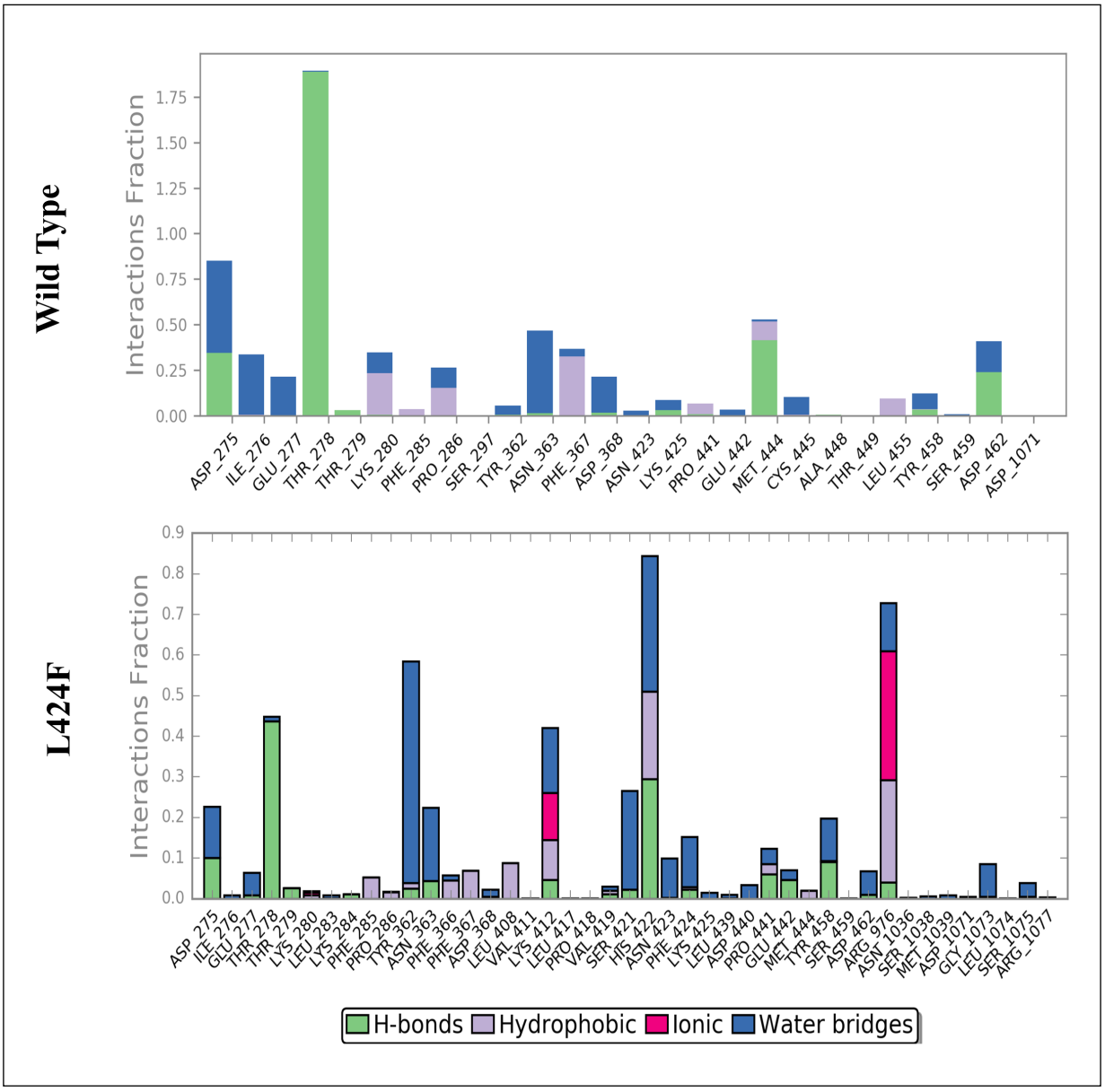

Figure 8. Hydrogen bonds observed between protein and ligand for the wildtype and mutant structures.

ferent *POLE* mutants now requires further clinical and experimental validation.

Conflicts of Interest

The authors declare no conflict of interest.

Authors' Contributions

Conceptualization, L.L., S.J.C. and A.M.A.; methodology, L.L., K.M. and A.M.A.; software, L.L. and K.M.; validation, A.A.H., and A.G.K.; formal analysis, L.L. and K.M.; investigation, S.B. and F.H.C.; resources, A.A.H.; data curation, L.L. and A.G.K.; writing - original draft preparation, L.L. and S.J.C.; writing - review and editing, A.M.A. and S.B.; visualization, A.A. and A.A.H.; supervision, K.M. and A.M.A.; funding acquisition, A.A.H. All authors have read and agreed to the published version of the manuscript.

Funding

This publication was supported by Qatar University, internal grant No. QUCP-CHS-2022-551. The findings achieved herein are solely the responsibility of the authors.

Ethics Approval

Not applicable.

Informed Consent

Not applicable.

References

1) Pursell ZF, Isoz I, Lundstrom EB, Johansson E, Kunkel TA. Yeast DNA Polymerase participates in leading-strand DNA replication. Science 2007; 317: 127-130.
2) Bulock CR, Xing X, Shcherbakova PV. DNA polymerase δ proofreads errors made by DNA polymerase ε. Proc Natl Acad Sci USA 2020; 117: 6035-6041.
3) Mur P, García-Mulero S, Del Valle J, Magraner-Pardo L, Vidal A, Pineda M, Cinnirella G, Martín-Ramos E, Pons T, López-Doriga A, Belhadj S, Feliubadaló L, Munoz-Torres PM, Navarro M, Grau E, Darder E, Llort G, Sanz J, Ramón Y Cajal T, Balmana J, Brunet J, Moreno V, Piulats JM, Matías-Guiu X, Sanz-Pamplona R, Aligué R, Capellá G, Lázaro C, Valle L. Role of POLE and POLD1 in familial cancer. Genet Med 2020; 22: 2089-2100.
4) Park VS, Pursell ZF. POLE proofreading defects: Contributions to mutagenesis and cancer. DNA Repair 2019; 76: 50-59.
5) Hodel KP, Sun MJS, Ungerleider N, Park VS, Williams LG, Bauer DL, Immethun VE, Wang J, Suo Z, Lu H, McLachlan JB, Pursell ZF. POLE mutation spectra are shaped by the mutant allele identity, its abundance, and mismatch repair status. Mol Cell 2020; 78: 1166-1177.
6) Wang F, Zhao Q, Wang YN, Jin Y, He MM, Liu ZX, Xu RH. Evaluation of POLE and POLD1 mutations as biomarkers for immunotherapy outcomes across multiple cancer types. JAMA Oncol 2019; 5: 1504-1506.
7) Cerami E, Gao J, Dogrusoz U, Gross BE, Sumer SO, Aksoy BA, Jacobsen A, Byrne CJ, Heuer ML, Larsson E, Antipin Y, Reva B, Goldberg AP, Sander C, Schultz N. The cBio cancer genomics portal: an open platform for exploring multidimensional cancer genomics. Cancer Discov 2012; 2: 401-404.
8) Gao J, Aksoy BA, Dogrusoz U, Dresdner G, Gross B, Sumer SO, Sun Y, Jacobsen A, Sinha R, Larsson E, Cerami E, Sander C, Schultz N. Integrative analysis of complex cancer genomics and clinical profiles sing the cBioPortal. Sci Signal 2013; 6: pl1.
9) Sigal DS, Miller HJ, Schram ED, Saven A. Beyond hairy cell: The activity of cladribine in other hematologic malignancies. Blood 2010; 116: 2884-2896.
10) Rammohan K, Coyle PK, Sylvester E, Galazka A, Dangond F, Grosso M, Leist TP. The Development of cladribine tablets for the treatment of multiple sclerosis: a comprehensive review. Drugs 2020; 80: 1901-1928.
11) DrugBank online: Cladribine. Accessed September 10, 2022. Available at: https://go.drugbank.com/drugs/DB00242.
12) Zhenchuk A, Lotfi K, Juliusson G, Albertioni F. Mechanisms of anti-cancer action and pharmacology of clofarabine. Biochem Pharmacol 2009; 78: 1351-1359.
13) Van Gool IC, Rayner E, Osse EM, Nout RA, Creutzberg CL, Tomlinson IPM, Church DN, Smit VTHBM, De Wind N, Bosse T, Drost M. Adjuvant treatment for *POLE* proofreading domain–mutant cancers: sensitivity to radiotherapy, chemotherapy, and nucleoside analogues. Clin Cancer Res 2018; 24: 3197-3203.
14) León-Castillo A, Britton H, McConechy MK, McAlpine JN, Nout R, Kommoss S, Brucker SY, Carlson JW, Epstein E, Rau TT, Bosse T, Church DN, Gilks CB. Interpretation of somatic POLE mutations in endometrial carcinoma. J Pathol 2020; 250: 323-335.
15) Imboden S, Nastic D, Ghaderi M, Rydberg F, Rau TT, Mueller MD, Epstein E, Carlson JW. Phenotype of POLE-mutated endometrial cancer. PLoS One 2019; 14: e0214318.
16) Cladribine: Uses, Interactions, Mechanism of action | DrugBank online. Drug Bank Online. Accessed on September 10, 2022.
17) Yu S, Shao H, Ban X, Zhang H, You Y, Zhou N, Mao X, Zhao H, Chen J, Lu Z. Detection of POLE subtypes in high-grade endometrioid carcinoma by basescope-ISH assay. Front Oncol 2019; 9: 831.
18) Shinbrot E, Henninger EE, Weinhold N, Covington KR, Göksenin AY, Schultz N, Chao H, Doddapaneni H, Muzny DM, Gibbs RA, Sander C, Pursell ZF, Wheeler DA. Exonuclease mutations in DNA polymerase epsilon reveal replication strand specific mutation patterns and human origins of replication. Genome Res 2014; 24: 1740-1750.
19) Meng B, Hoang LN, McIntyre JB, Duggan MA, Nelson GS, Lee CH, Köbel M. POLE exonuclease domain mutation predicts long progression-free survival in grade 3 endometrioid carcinoma of the endometrium. Gynecol Oncol 2014; 134: 15-19.
20) Loganathan L, Gopinath K, Sankaranarayanan VM, Kukreti R, Rajendran K, Lee JK, Muthusamy K. Computational and pharmacogenomic insights on hypertension treatment: rational drug design and optimization strategies. Curr Drug Targets 2019; 21: 18-33.
21) Loganathan L, Kuriakose BB, Mushfiq S, Muthusamy K. Mechanistic insights on nsSNPs on binding site of renin and cytochrome P450 proteins: a computational perceptual study for pharmacogenomics evaluation. J Cell Biochem 2021; 122: 1460-1474.
22) Halgren TA. Identifying and characterizing binding sites and assessing druggability. J Chem Inf Model 2009; 49: 377-389.
23) Schrödinger. Glide | Schrödinger. Schrödinger Release 2019; 4.
24) Friesner RA, Murphy RB, Repasky MP, Frye LL, Greenwood JR, Halgren TA, Sanschagrin PC, Mainz DT. Extra precision glide: Docking and scoring incorporating a model of hydrophobic enclosure for protein-ligand complexes. J Med Chem 2006; 49: 6177-6196.
25) Swetha RG, Ramaiah S, Anbarasu A. Molecular dynamics studies on D835N mutation in FLT3 - Its

impact on FLT3 protein structure. J Cell Biochem 2016; 117: 1439-1445.
26) Katoh K, Misawa K, Kuma Kichi, Miyata T. MAFFT. A novel method for rapid multiple sequence alignment based on fast Fourier transform. Nucleic Acids Res 2002; 30: 3059-3066.
27) Kearse M, Moir R, Wilson A, Stones-Havas S, Cheung M, Sturrock S, Buxton S, Cooper A, Markowitz S, Duran C, Thierer T, Ashton B, Meintjes P, Drummond A. Geneious Basic: An integrated and extendable desktop software platform for the organization and analysis of sequence data. Bioinformatics 2012; 28: 1647-1649.
28) Desmond | Schrödinger. Maestro, Schrodinger 2019; -4. Accessed on September 10, 2022. Available at: https://www.schrodinger.com/products/desmond.
29) Singh KhD, Kirubakaran P, Nagarajan S, Sakkiah S, Muthusamy K, Velmurgan D, Jeyakanthan J. Homology modeling, molecular dynamics, e-pharmacophore mapping and docking study of Chikungunya virus nsP2 protease. J Mol Model 2012; 18: 39-51.
30) Ashkenazy H, Abadi S, Martz E, Chay O, Mayrose I, Pupko T, Ben-Tal N. ConSurf 2016: an improved methodology to estimate and visualize evolutionary conservation in macromolecules. Nucleic Acids Res 2016; 44: 344-350.
31) Quan L, Lv Q, Zhang Y. STRUM: Structure-based prediction of protein stability changes upon single-point mutation. Bioinformatics 2016; 32: 2936-2946.